# A PENALTY FINITE ELEMENT METHOD FOR NON–NEWTONIAN CREEPING FLOWS

*Ramon CODINA, Miguel CERVERA and Eugenio OÑATE*

*Escola Tècnica Superior d'Enginyers de Camins, Canals i Ports*
*Universitat Politècnica de Catalunya*
*Gran Capità s/n, Mòdul C1, 08034 Barcelona, Spain*

## SUMMARY

In this paper we present an iterative penalty finite element method for viscous non-Newtonian creeping flows. The basic idea is solving the equations for the difference between the exact solution and the solution obtained in the last iteration by the penalty method. For the case of Newtonian flows, one can show that for sufficiently small penalty parameters the iterates converge to the incompressible solution. The objective of the present work is to show that the iterative penalization can be coupled with the iterative scheme used to deal with the nonlinearity arising from the constitutive law of non-Newtonian fluids. Some numerical experiments are conducted in order to assess the performance of the approach for fluids whose viscosity obeys the power law.

## INTRODUCTION

The use of the penalty method for the finite element solution of incompressible flow problems has attracted the attention of many researchers. Its popularity is mainly due to the fact that it reduces the number of nodal unknowns of the problem. On the other hand, if the pure incompressible mixed velocity-pressure formulation is adopted, the element stiffness matrix of the discrete finite element problem has zero diagonal terms. Most of the standard finite element direct solvers use the elements of the diagonal as pivots [31]. In this case, renumbering algorithms have to be modified in order to prevent the appearence of zeroes in the diagonal of the assembled matrix when reducing the equations in the solution process. This results in the increase of the bandwidth of the global matrix. This problem is circumvented if the incompressibility constraint is penalized.

The main drawback of the penalty method is the ill-conditioning of the stiffness matrix when the penalty parameter is very small. For Newtonian flows, a fairly wide range of values of this parameter are known to yield good results (that is, the incompressibility equation is sufficiently well approximated) and to be easily handled if direct solvers are employed. Experience shows that the range $\epsilon = 10^{-6}\mu^{-1}$ to $\epsilon = 10^{-9}\mu^{-1}$ is recommended [15], [30]. Here and below, $\epsilon$ denotes the penalty number and $\mu$ the dynamical viscosity of the fluid. Two questions arise. The first is what happens for non-Newtonian flows. In this case, the viscosity may vary several orders of magnitude in the fluid domain, especially if the physical properties of the material are considered to be thermally sensitive. The above rule for choosing the penalty parameter has to be applied using the smallest value of the viscosity (in order to avoid ill-conditioning), which is unknown before the calculation. Besides that, the incompressibility constraint will be excessively relaxed in the high viscosity zones. Another question to be considered is whether iterative solvers can be safely used or not. Usually, their convergence

is very sensitive to the condition number of the stiffness matrix, which grows as the penalty parameter decreases. When the effect of the non-constant viscosity is present and iterative solvers are used the behavior of the standard penalty method is certainly disappointing [3].

The objective of this paper is to present an iterative penalty finite element method whose basic motivation is alleviating the problems mentioned above. The incompressibility equation is penalized in each iteration but the residual of the previous iterate is added as a forcing term. For the case of the Stokes problem with constant viscosity, the convergence properties of the method are proved in a previous work [5] and are also briefly stated here. The interesting issue is what happens when the iterative penalization is coupled with the iterative procedure due to the nonlinearity of the problem. The case in which this nonlinearity comes from the momentum equation (Navier-Stokes problem) is studied in detail in Reference [5] when the Picard and the Newton-Raphson algorithms are employed. Our purpose now is to present the method in the general framework of thermally coupled flows of non-linear fluids. We will focus our attention in non-Newtonian creeping flows. In the last part of the paper, some numerical experiments concerning the well known 4:1 plane extrusion test for a fluid whose viscosity obeys the power law are presented.

## BASIC EQUATIONS FOR THERMALLY COUPLED QUASI-NEWTONIAN FLOWS

*Conservation equations and constitutive model*

In what follows, we will only consider low Reynolds number steady-state flows. In this case, the time evolution and inertial terms in the Navier-Stokes equations can be neglected. The problem to be solved is to find a velocity field $\mathbf{u}$ and a pressure $p$ such that

$$-2\nabla \cdot (\mu\varepsilon(\mathbf{u})) + \nabla p = \rho\mathbf{f} \quad \text{in } \Omega \qquad (1)$$
$$\nabla \cdot \mathbf{u} = 0 \quad \text{in } \Omega \qquad (2)$$

where $\nabla \cdot (\cdot)$ is the divergence operator, $\nabla(\cdot)$ the gradient operator, $\varepsilon(\mathbf{u})$ the symmetric part of $\nabla\mathbf{u}$, $\rho$ the material density, $\mathbf{f}$ the exterior body force and $\Omega$ is a bounded domain in $\mathbb{R}^{N_{sd}}$ ($N_{sd} = 2$ or $3$). Whenever the viscosity $\mu$ is constant, Eqn. (1) can be simplified using Eqn. (2). The viscous term can be written as $-\mu\Delta\mathbf{u}$, where $\Delta(\cdot)$ is the Laplacian operator. However, the expression $-2\nabla \cdot (\mu\varepsilon(\mathbf{u}))$ will be kept since we are interested in non-constant viscosities.

Eqn. (1) comes from the conservation of momentum assuming the constitutive law of generalized Newtonian fluids

$$\boldsymbol{\sigma} = -p\mathbf{I} + 2\mu\varepsilon, \qquad (3)$$

$\boldsymbol{\sigma}$ being the stress tensor and $\mathbf{I}$ the unit tensor. In general, $\mu$ will be a function of the invariants of $\varepsilon$. Eqn. (2) states the conservation of mass for an incompressible material. In this case, the mechanical and thermal behavior of the fluid is completely described by Eqns. (1), (2) and the energy balance, that leads to the convection-diffusion equation for the temperature field $\theta$:

$$\rho c\mathbf{u} \cdot \nabla\theta - k\Delta\theta = Q \qquad (4)$$

Here, we have considered a constant and isotropic thermal conductivity $k$. The constant $c$ in Eqn. (4) is the specific heat and $Q$ is the source term. Only the source coming from the mechanical dissipation into heat will be taken into account:

$$Q = \boldsymbol{\sigma} : \varepsilon = 2\mu\varepsilon(\mathbf{u}) : \varepsilon(\mathbf{u}) \qquad (5)$$

2

where the symbol : denotes the dyadic product of two tensors. In Eqn. (5) we have used the fact that $\mathbf{I} : \boldsymbol{\varepsilon}(\mathbf{u}) = \nabla \cdot \mathbf{u} = 0$.

Boundary conditions have to be appended to problem (1)–(2)–(4). Let $\Gamma$ be the boundary of $\Omega$, splitted into two sets of disjoint components $\Gamma = \Gamma_{du} \cup \Gamma_{nu}$ and $\Gamma = \Gamma_{dt} \cup \Gamma_{nt}$. Let $\mathbf{n}$ be the unit vector normal to $\Gamma$, $\mathbf{u}_0$ the velocity prescribed on $\Gamma_{du}$, $\mathbf{t}_0$ the prescribed traction on $\Gamma_{nu}$, $\theta_0$ the given temperature on $\Gamma_{dt}$ and $\alpha, g,$ and $\theta_1$ the thermal conduction coefficient, the prescribed heat flux and the ambient temperature on $\Gamma_{nt}$, respectively. The boundary conditions to be considered are

$$\mathbf{u} = \mathbf{u}_0 \quad \text{on } \Gamma_{du} \tag{6}$$

$$\mathbf{n} \cdot \boldsymbol{\sigma} = \mathbf{t}_0 \quad \text{on } \Gamma_{nu} \tag{7}$$

$$\theta = \theta_0 \quad \text{on } \Gamma_{dt} \tag{8}$$

$$-k\mathbf{n} \cdot \nabla\theta = g + \alpha(\theta - \theta_1) \quad \text{on } \Gamma_{nt} \tag{9}$$

In order to write the weak form of problem (1),(2),(4),(6)–(9), let $\mathcal{V}_u, \mathcal{V}_p$ and $\mathcal{V}_t$ be the spaces of trial functions for the velocity, the pressure and the temperature, respectively, defined by:

$$\mathcal{V}_u = \{\mathbf{v} \in H^1(\Omega)^N : \mathbf{v}|_{\Gamma_{du}} = \mathbf{u}_0\}$$

$$\mathcal{V}_p = \{q \in L^2(\Omega) : \int_\Omega q d\Omega = 0 \text{ if } \Gamma_{du} = \Gamma\}$$

$$\mathcal{V}_t = \{\eta \in H^1(\Omega) : \eta|_{\Gamma_{dt}} = \theta_0\}$$

The spaces of weighting functions $\mathcal{W}_u, \mathcal{W}_p$ and $\mathcal{W}_t$ are

$$\mathcal{W}_u = \{\mathbf{v} \in H^1(\Omega)^N : \mathbf{v}|_{\Gamma_{du}} = \mathbf{0}\}$$

$$\mathcal{W}_p = L^2(\Omega)$$

$$\mathcal{W}_t = \{\eta \in H^1(\Omega) : \eta|_{\Gamma_{dt}} = 0\}$$

Having introduced all this notation, the weak form of the problem we consider is: find a velocity field $\mathbf{u} \in \mathcal{V}_u$, a pressure $p \in \mathcal{V}_p$ and a temperature $\theta \in \mathcal{V}_t$ such that

$$2\int_\Omega \mu\boldsymbol{\varepsilon}(\mathbf{u}) : \boldsymbol{\varepsilon}(\mathbf{v})d\Omega - \int_\Omega p\nabla \cdot \mathbf{v}d\Omega = \rho\int_\Omega \mathbf{f} \cdot \mathbf{v}d\Omega + \int_{\Gamma_{nu}} \mathbf{t}_0 \cdot \mathbf{v}d\Gamma \tag{10}$$

$$\int_\Omega q\nabla \cdot \mathbf{u}d\Omega = 0 \tag{11}$$

$$k\int_\Omega \nabla\theta \cdot \nabla\eta d\Omega + \rho c \int_\Omega (\mathbf{u} \cdot \nabla\theta)\eta d\Omega = 2\int_\Omega \mu\boldsymbol{\varepsilon}(\mathbf{u}) : \boldsymbol{\varepsilon}(\mathbf{u})\eta d\Omega + \int_{\Gamma_{nt}} [g + \alpha(\theta - \theta_1)]\eta d\Gamma \tag{12}$$

for all $\mathbf{v} \in \mathcal{W}_u$, $q \in \mathcal{W}_p$ and $\eta \in \mathcal{W}_t$.

The constitutive law of the fluid will enter problem (10)–(12) through an equation relating the viscosity with the temperature and the invariants of $\boldsymbol{\varepsilon}(\mathbf{u})$. Let us write, symbolically:

$$\mu = \mu(\theta, \boldsymbol{\varepsilon}(\mathbf{u})) \tag{13}$$

At the end of the paper we will present some numerical experiments for a particular case of (13), namely, for the power law with an exponential-type thermal dependence.

*Finite element discretization*

Let $\{\Omega_e\}$ be a finite element discretization of the domain $\Omega$, with subscript $e$ ranging from 1 to the number of elements $N_{el}$. For each element, denote by $N_{nu}, N_{np}$ and $N_{nt}$ the number of nodes with velocity, pressure and temperature degrees of freedom, respectively. The discrete version of problem (10)–(12) leads to the following algebraic system:

$$\mathbf{K}(\mu)\mathbf{U} - \mathbf{G}\mathbf{P} = \mathbf{F}_u \tag{14}$$

$$\mathbf{G}^T\mathbf{U} = \mathbf{F}_p \tag{15}$$

$$\mathbf{H}(\mathbf{u})\mathbf{\Theta} = \mathbf{F}_t(\mu, \mathbf{u}) \tag{16}$$

We have explicitly indicated the dependence of the matrices and vectors in the above equations on the viscosity and the velocity. Capital letters $\mathbf{U}, \mathbf{P}$ and $\mathbf{\Theta}$ denote the vector of nodal unknowns of the corresponding lower case variables. The expression of the matrices $\mathbf{K}$, $\mathbf{G}$ and $\mathbf{H}$ and the vectors $\mathbf{F}_u$ and $\mathbf{F}_t$ can be consulted in any standard finite element text book (see, e.g. [6], [14], [31]). The vector $\mathbf{F}_p$ comes from the imposition of the Dirichlet boundary condition (6) for the velocity field.

Consider first the case in which the viscosity $\mu$ does not depend on the temperature $\theta$. Under this assumption, Eqns. (14) and (15) are uncoupled with Eqn. (16), that can be solved once $\mathbf{U}$ is known. If the viscosity $\mu$ is constant (Newtonian fluid), it is well known that the discrete velocity space $\mathcal{V}_{u,h}$ and pressure space $\mathcal{V}_{p,h}$ must satisfy the discrete Babuška-Brezzi (BB) stability condition [2]. When the viscosity depends on the invariants of the strain-rate tensor $\varepsilon(\mathbf{u})$, the question is whether this condition will be sufficient for assessing stability and convergence of the finite element scheme. In Reference [1], it was proved that for the case in which the viscosity obeys the power law or the Carreau model, stable and convergent velocity-pressure pairs for the Stokes problem with $\mu$ constant are also stable for the nonlinear case. Concerning the convergence of the method, let $h$ be the diameter of $\{\Omega_e\}$ and suppose that the rate of convergence for the velocity is of order $h^m$ for Newtonian flows. Assume now that $\mu$ satisfies the power law with rate of sensitivity $r$, with $0 < r < 1$. Then, the rate of convergence for the velocity will be of order $h^{mr}$. For the Carreau model, the same rate of convergence as for the constant viscosity case can be obtained. See Reference [1] for details.

Based on the results stated above, finite element interpolations for the velocity and the pressure that are known to satisfy the discrete Babuška-Brezzi condition have been employed. See References [14], [31] for a fairly complete description of available interpolations and Reference [11] for the analysis of the elements. As will be shown later, we will be interested in discontinuous pressure interpolations. Table 1 shows some of the elements we have programmed for the Stokes problem. Elements $Q1/P0$, $Q2/P1$ and $Q2^-/P0$ are quadrilateral in 2D and hexahedral in 3D. The others are triangular in 2D and tetrahedral in 3D. The pressure nodes are always placed in the interior of the element. As usual, the interpolation is defined in the parent domain (reference element). The isoparametric mapping to the physical domain is then constructed using the velocity shape functions.

*Remarks*

(1) The element $Q1/P0$ does not satisfy the BB condition in its primitive form. Iterative stabilization methods [10] or finite element discretizations in macroelements composed of this element [25] have to be used in order to obtain a stable scheme.

(2) The element $Q2/P1$, first proposed in Reference [20], is known to yield very good results for incompressible flow problems [9]. We have used this element in the numerical examples presented later. We have also obtained excellent answers with the $P2^+/P1$ element. Both the $Q2/P1$ and the $P2^+/P1$ elements are known to have optimal rates of convergence. For

sufficiently smooth solutions of the continuous problem, the rate of convergence is of order $h^3$ for the velocity and of order $h^2$ for the pressure (in the $L^2$ norm) [11].

(3) Concerning the implementation of piecewise linear pressures, two options are possible. If $s = (s_1, s_2, s_3)$ (in 3D) are the coordinates of the parent domain of the elements, the first choice is to place $N_{sd} + 1 = 4$ nodes within the elements, with coordinates $s_j$, $j = 1, 2, 3, 4$, and construct shape functions $N_i(s)$, $i = 1, 2, 3, 4$, such that $N_i(s_j) = \delta_{ij}$ (the Kronecker symbol) for $i, j = 1, 2, 3, 4$. Then, if the pressure is interpolated as $p(s) = \sum_{i=1}^{4} N_i(s) p_i$, the coefficients $p_i$, $i = 1, 2, 3, 4$, have the meaning of being the nodal values of the pressure. A simpler option is to interpolate $p$ as $p(s) = p_0 + s_1 p_1 + s_2 p_2 + s_3 p_3$. Now, $p_0$ is the value of the pressure for $s_1 = s_2 = s_3 = 0$ and $p_1, p_2$ and $p_3$ are its first derivatives. In our computations, we have found no difference in the numerical results using both approaches.

Up to now, we have described the velocity and pressure interpolations. For the temperature, we use the same interpolation as for the components of the velocity. Thus, $N_{nt} = N_{nu}$.

## THE ITERATIVE PENALTY METHOD

*Description of the method and convergence properties for Newtonian flows*

For simplicity, we will assume now the case in which $u_0 = 0$, $\mu$ is constant and $\Gamma_{nu}$ is the empty set. The matrix form of the problem is now:

$$\mathbf{K}(\mu)\mathbf{U} - \mathbf{GP} = \mathbf{F}_u \tag{17}$$

$$\mathbf{G}^T \mathbf{U} = \mathbf{0} \tag{18}$$

Let $\mathbf{M}$ be any positive definite (not necessarily symmetric) $n_2 \times n_2$ matrix, $n_2$ being the total number of pressure unknowns. In particular, $\mathbf{M}$ can be taken as the Gramm matrix whose components are the inner products of the pressure shape functions $N_p$:

$$M_{ij} = \int_{\Omega} N_p^{(i)} N_p^{(j)} d\Omega \tag{19}$$

where the superscripts $i$ and $j$ refer to the pressure node. If $\epsilon$ is a small number, the penalty method applied to problem (17)–(18) leads to the following algebraic system:

$$\mathbf{K}(\mu)\mathbf{U}^{\epsilon(1)} - \mathbf{GP}^{\epsilon(1)} = \mathbf{F}_u \tag{20}$$

$$\mathbf{G}^T \mathbf{U}^{\epsilon(1)} + \epsilon \mathbf{MP}^{\epsilon(1)} = \mathbf{0} \tag{21}$$

Let $\mathbf{U} = \mathbf{U}^{\epsilon(1)} + \delta\mathbf{U}$ and $\mathbf{P} = \mathbf{P}^{\epsilon(1)} + \delta\mathbf{P}$ be the solution of problem (17)–(18), where $\mathbf{U}^{\epsilon(1)}$ and $\mathbf{P}^{\epsilon(1)}$ is the solution of problem (20)–(21). Substracting Eqn. (20) from (17) and Eqn. (21) from (18) one finds that

$$\mathbf{K}(\mu)\delta\mathbf{U} - \mathbf{G}\delta\mathbf{P} = \mathbf{0} \tag{22}$$

$$\mathbf{G}^T \delta\mathbf{U} = \epsilon \mathbf{MP}^{\epsilon(1)} \tag{23}$$

This problem can be solved again using the penalty method. Let $\delta\mathbf{U}^{\epsilon}$ and $\delta\mathbf{P}^{\epsilon}$ be the penalized solution and define $\mathbf{U}^{\epsilon(2)} = \mathbf{U}^{\epsilon(1)} + \delta\mathbf{U}^{\epsilon}$ and $\mathbf{P}^{\epsilon(2)} = \mathbf{P}^{\epsilon(1)} + \delta\mathbf{P}^{\epsilon}$. We will have that:

$$\mathbf{K}(\mu)\mathbf{U}^{\epsilon(2)} - \mathbf{GP}^{\epsilon(2)} = \mathbf{F}_u \tag{24}$$

$$\mathbf{G}^T \mathbf{U}^{\epsilon(2)} + \epsilon \mathbf{MP}^{\epsilon(2)} = \epsilon \mathbf{MP}^{\epsilon(1)} \tag{25}$$

Applying inductively the same reasoning used to arrive at (24)-(25) the following algorithm is obtained:

*Given* $\mathbf{P}^{\epsilon(0)}$, *for* $i = 1, 2, ...$ *find* $\mathbf{U}^{\epsilon(i)}$ *and* $\mathbf{P}^{\epsilon(i)}$ *such that*

$$\mathbf{K}(\mu)\mathbf{U}^{\epsilon(i)} - \mathbf{G}\mathbf{P}^{\epsilon(i)} = \mathbf{F}_u \tag{26}$$

$$\mathbf{G}^T\mathbf{U}^{\epsilon(i)} + \epsilon\mathbf{M}\mathbf{P}^{\epsilon(i)} = \epsilon\mathbf{M}\mathbf{P}^{\epsilon(i-1)} \tag{27}$$

This is the discrete version of the algorithm proposed and analysed in Reference [5] for the Stokes problem. It should be remarked that the initial guess $\mathbf{P}^{\epsilon(0)}$ must be such that the associated pressure (interpolated from these nodal values) have zero mean value.

*Remarks*

(1) Algorithm (26)-(27) may be viewed as a variant of the Augmented Lagrangian method (see, e.g. References [12], [26]) provided that Uzawa's algorithm is used to update the pressure. This was implicitly done in early works whose basic motivation was also the computational problems encountered when small penalties are used (for example, the method was applied in linear incompressible Elasticity in Reference [24] and the discrete algebraic system was considered in Reference [8]. See also Reference [33]). An important difference between our approach and the Augmented Lagrangian method is that, as will be seen below, we *will not* require the matrix $\mathbf{K}$ to be symmetric (although it certainly is, for the problem we consider) and thus an associated minimization problem is not needed for deriving (26)-(27). For an application of the Augmented Lagrangian method for non-Newtonian fluids, see Reference [16].

(2) The residual out-of-balance argument used to arrive at (26)-(27) is completely general and has physical meaning for nonlinear cases, either if the nonlinearity comes from the momentum equations (Navier-Stokes problem) or from the constitutive law of the material. The step from problem (20)-(21) to problem (22)-(23) may be applied in nonlinear problems as well, although in these cases $\delta\mathbf{U}$ and $\delta\mathbf{P}$ will be the solution of a nonlinear problem that in turn has to be linearized. Our leading idea is trying to converge in this process to the true incompressible solution. See the Appendix.

(3) There are possibly many ways for 're-discovering' algorithm (26)-(27). Another one is to introduce a false transient for the pressure (not for the momentum equation) assuming the fluid to be slightly compressible and then to discretize the temporal derivative using the backward Euler scheme. Except for this discretization, this is nothing but the artificial compressibility method introduced by Chorin [4]. The penalty parameter $\epsilon$ in this case would be the inverse of $c^2\Delta t$, where $c$ is the speed of sound in the fluid and $\Delta t$ the time step. See Reference [13] for further discussion.

(4) Looking at problem (20)-(21) we see that the *discrete* incompressibility constraint has been penalized. The pressure interpolation is thus independent of the finite element velocity space and stable velocity-pressure interpolations can be used. On the other hand, if one starts penalizing the continuous incompressibility constraint and then eliminating the pressure in the momentum equations, the associated pressure space is determined by the velocity space. In general, the resulting velocity-pressure pair will not satisfy the BB stability condition and in order to obtain stable or semi-stable schemes, reduced or selective integration techniques have to be employed [21], [22], [32]. We will not consider these methods in this paper. For further discussion, see References [7], [9], [17], [19], [22].

Although expressions (26)-(27) will be kept in what follows, their implementation uses the fact that the pressure interpolation is discontinuous. This allows to eliminate the pressure degrees of freedom, thus making the method much more efficient from the computational point of

view. For discontinuous pressures, Eqn. (27) holds for each element. If we denote by superscript $e$ the element arrays, we will have that

$$\mathbf{G}^{(e)T}\mathbf{U}^{(e)\epsilon(i)} + \epsilon\mathbf{M}^{(e)}\mathbf{P}^{(e)\epsilon(i)} = \epsilon\mathbf{M}^{(e)}\mathbf{P}^{(e)\epsilon(i-1)} \tag{28}$$

and hence

$$\mathbf{P}^{(e)\epsilon(i)} = \mathbf{P}^{(e)\epsilon(i-1)} - \frac{1}{\epsilon}\mathbf{M}^{(e)-1}\mathbf{G}^{(e)T}\mathbf{U}^{(e)\epsilon(i)} \tag{29}$$

Let $\mathcal{A}$ denote the standard finite element assembly operator. From (26) and (29) we have that:

$$\left[\mathbf{K}(\mu) + \frac{1}{\epsilon}\mathcal{A}_{e=1}^{N_{el}}\left(\mathbf{G}^{(e)}\mathbf{M}^{(e)-1}\mathbf{G}^{(e)T}\right)\right]\mathbf{U}^{\epsilon(i)} = \mathbf{F}_u + \mathbf{G}\mathbf{P}^{\epsilon(i-1)} \tag{30}$$

Once $\mathbf{U}^{\epsilon(i)}$ is found by solving Eqn. (30), the pressure nodal values can be computed for each element from the expression (29). It should be remarked that the matrix of the system (30) has to be factored only once for Newtonian flows and that the inversion of $\mathbf{M}^{(e)}$ is trivial (it is a $(N_{sd}+1) \times (N_{sd}+1)$ matrix if linear pressures are used).

We now proceed to analyse the convergence of the iterates $\mathbf{U}^{\epsilon(i)}, \mathbf{P}^{\epsilon(i)}$, solution of problem (26)–(27), to the pure incompressible solution $\mathbf{U}, \mathbf{P}$ of problem (17)–(18). Our objective is to use arguments as simple as possible, only involving linear algebra concepts (see Reference [5] for a more abstract approach). Let $N_{fn}$ be the total number of free nodes of the finite element mesh with velocity degrees of freedom. Define $n_1 = N_{sd} \times N_{fn}$ and $n_2 = N_{el} \times N_{np}$. We will have that $\mathbf{U}^{\epsilon(i)} \in \mathbb{R}^{n_1}$ and $\mathbf{P}^{\epsilon(i)} \in \mathbb{R}^{n_2}$. It is well known that $\mathbf{K}(\mu)$ is a symmetric and positive-definite $n_1 \times n_1$ matrix, with components proportional to $\mu$. We will not need its symmetry but only its positive-definiteness and its continuity (it defines a linear mapping in $\mathbb{R}^{n_1}$). Thus, there exist positive constants $C_1$ and $C_2$ such that

$$\begin{aligned} C_1\mu\|\mathbf{V}_1\|^2 &\leq \mathbf{V}_1^T\mathbf{K}(\mu)\mathbf{V}_1 \\ \mathbf{V}_1^T\mathbf{K}(\mu)\mathbf{V}_2 &\leq C_2\mu\|\mathbf{V}_1\|\|\mathbf{V}_2\| \end{aligned} \tag{31}$$

where $\mathbf{V}_1, \mathbf{V}_2 \in \mathbb{R}^{n_1}$ and $\|\cdot\|$ denotes the Euclidian norm in $\mathbb{R}^{n_1}$ or $\mathbb{R}^{n_2}$. For the $n_1 \times n_2$ matrix $\mathbf{G}$, we assume that the following condition holds: for each $\mathbf{Q} \in \mathbb{R}^{n_2}$ there exists a $\mathbf{V} \in \mathbb{R}^{n_1}$, $\mathbf{V} \neq 0$, such that

$$\mathbf{V}^T\mathbf{G}\mathbf{Q} \geq C_3\|\mathbf{V}\|\|\mathbf{Q}\| \tag{32}$$

for a certain positive constant $C_3$ independent of the mesh diameter $h$. Condition (32) is the discrete form of the BB stability condition. See Reference [2] for an equivalent formulation.

The final ingredient we need is the fact that $\mathbf{M}$ is also a positive-definite matrix. Thus, there exist positive constants $C_4$ and $C_5$ such that

$$\begin{aligned} C_5\|\mathbf{Q}_1\|^2 &\leq \mathbf{Q}_1^T\mathbf{M}\mathbf{Q}_1 \\ \mathbf{Q}_1^T\mathbf{M}\mathbf{Q}_2 &\leq C_4\|\mathbf{Q}_1\|\|\mathbf{Q}_2\| \end{aligned} \tag{33}$$

for any $\mathbf{Q}_1, \mathbf{Q}_2 \in \mathbb{R}^{n_2}$.

Substracting now Eqn. (17) from (26) and Eqn. (18) from (27) we obtain:

$$\mathbf{K}(\mu)(\mathbf{U} - \mathbf{U}^{\epsilon(i)}) - \mathbf{G}(\mathbf{P} - \mathbf{P}^{\epsilon(i)}) = 0 \tag{34}$$

$$\mathbf{G}^T(\mathbf{U} - \mathbf{U}^{\epsilon(i)}) + \epsilon\mathbf{M}(\mathbf{P}^{\epsilon(i-1)} - \mathbf{P}^{\epsilon(i)}) = 0 \tag{35}$$

On the other hand, from conditions (33) we see that

$$0 \leq (P - P^{\epsilon(i)})^T M(P - P^{\epsilon(i)})$$
$$= (P - P^{\epsilon(i)})^T M(P - P^{\epsilon(i-1)}) + (P - P^{\epsilon(i)})^T M(P^{\epsilon(i-1)} - P^{\epsilon(i)})$$

and hence

$$(P - P^{\epsilon(i)})^T M(P^{\epsilon(i)} - P^{\epsilon(i-1)}) \leq (P - P^{\epsilon(i)})^T M(P - P^{\epsilon(i-1)}) \tag{36}$$

Multiplying Eqn. (34) by $U - U^{\epsilon(i)}$ and Eqn. (35) by $P - P^{\epsilon(i)}$ and using inequalities (31), (33) and (36) we find that

$$C_1 \mu \|U - U^{\epsilon(i)}\|^2 \leq (U - U^{\epsilon(i)})^T K(\mu)(U - U^{\epsilon(i)})$$
$$= (U - U^{\epsilon(i)})^T G(P - P^{\epsilon(i)})$$
$$= \epsilon(P - P^{\epsilon(i)})^T M(P^{\epsilon(i)} - P^{\epsilon(i-1)})$$
$$\leq \epsilon C_4 \|P - P^{\epsilon(i)}\| \|P - P^{\epsilon(i-1)}\| \tag{37}$$

Let $V \in \mathbb{R}^{n_1}$ be such that condition (32) holds for $Q = P - P^{\epsilon(i)}$. Multiplying Eqn. (34) by this $V$ and using (31) we obtain

$$C_3 \|V\| \|P - P^{\epsilon(i)}\| \leq V^T G(P - P^{\epsilon(i)})$$
$$= V^T K(\mu)(U - U^{\epsilon(i)})$$
$$\leq C_2 \mu \|V\| \|U - U^{\epsilon(i)}\| \tag{38}$$

The combination of inequalities (37) and (38) leads to

$$\|U - U^{\epsilon(i)}\| \leq (\epsilon \mu C) \frac{C_3}{\mu C_2} \|P - P^{\epsilon(i-1)}\| \tag{39}$$

$$\|P - P^{\epsilon(i)}\| \leq (\epsilon \mu C) \|P - P^{\epsilon(i-1)}\| \tag{40}$$

where we have defined

$$C = \frac{C_2^2 C_4}{C_1 C_3^2}$$

Applying repeatedly inequalities (39) and (40) we finally get

$$\|U - U^{\epsilon(i)}\| \leq (\epsilon \mu C)^i \frac{C_3}{\mu C_2} \|P - P^{\epsilon(0)}\| \tag{41}$$

$$\|P - P^{\epsilon(i)}\| \leq (\epsilon \mu C)^i \|P - P^{\epsilon(0)}\| \tag{42}$$

From these relations (41) and (42) we obtain the following Theorem: *there exists a constant $C$ such that if $\bar{\epsilon} = \epsilon \mu C < 1$ then the iterates solution of problem (26)–(27) converge to the solution of problem (17)–(18). Moreover, convergence is linear with $\bar{\epsilon}$.*

Let us now discuss some practical consequences of this result. The obvious one is that larger penalty parameters $\epsilon$ can be used for the iterative algorithm (26)–(27) than for the standard penalty method. The incompressibility constraint can be approximated up to any given tolerance with a given $\epsilon$ provided that $\bar{\epsilon} < 1$. The price to be paid is that several iterations of (26)–(27) might be required. However, for large problems this is compensated by the reduction of the number of nodal unknowns with respect to the pure mixed formulation, as explained above. This reduction is especially important in 3D problems [23].

It is interesting to observe that convergence is governed by the parameter $\bar{\epsilon}$, which is proportional to the viscosity $\mu$. This explains why $\epsilon$ must be taken proportional to $\mu^{-1}$, since what provides an idea of how well the incompressibility constraint will be approximated is $\bar{\epsilon}$, and not $\epsilon$ itself. Of course, this comment can also be applied to the classical penalty method (observe that the first pass in (26)–(27) is nothing but the standard penalty method), and must be kept in mind when one deals with non-constant viscosities.

In practical problems, we have encountered two cases in which the the standard penalty method cannot be applied and the iterative penalization just described is mandatory. The first is the one discussed in this work, concerning non-Newtonian flows with variable viscosity. In the numerical examples presented below, it will be seen that the viscosity varies several orders of magnitude in the fluid domain. If a reference viscosity $\mu_0$ is chosen *a priori* for determining a suitable value of $\epsilon$, it is not known whether this penalty parameter will yield a sufficiently accurate satisfaction of the incompressibility constraint or to ill-conditioning of the final stiffness matrix. We will insist on this point later. Perhaps another case in which the importance of the variable viscosity is more clear is when the pseudo-concentration method is used to follow free surfaces of creeping flows [27], [28]. The idea of the method is to discretize the whole domain that can be filled by the fluid assuming that it is occupied either by the fluid itself or by a fictious material. The physical properties of this fictious material have to be such that the effect of its motion upon the real fluid can be neglected. In particular, its viscosity must be much smaller than the real one (5 or 6 orders of magnitude is recommended in References [27], [28]). In our numerical experiments using this method we have found that the standard penalty method leads either to an ill-conditioned stiffness matrix or to a completely unacceptable approximation of the incompressibility constraint, whereas good results can be obtained using the iterative penalization proposed here.

Another issue to be considered is the use of iterative schemes to solve the algebraic system of equations. We have conducted some numerical tests for the Stokes problem using the conjugate gradient method. Due to the high condition number of the final stiffness matrix (see Eqn. (30)), we have found the standard penalty method unfeasible from the practical point of view. Research is currently being done in order to determine ranges of $\epsilon$ for the iterative penalty method that are a compromise between the approximation of the incompressibility constraint (within a reasonable number of iterations) and the rate of convergence of the conjugate gradient method.

*Iterative algorithm for thermally coupled non-Newtonian flows*

In order to solve the coupled nonlinear system of equations (14)–(16) we use a block iterative algorithm. Let $\mu^{(k,l)}$ denote the viscosity function when the temperature is known at iteration $k$ and the velocity at iteration $l$. Let $TOL$ be a given tolerance. We check convergence using the criterion $\|\mathbf{U}^{(i)} - \mathbf{U}^{(i-1)}\| < TOL\|\mathbf{U}^{(i)}\|$. The iterative scheme used is the following:

- Initialise $\mu^{(0,0)}$, $\mathbf{P}^{(0)}$, $\mathbf{\Theta}^{(0)}$
- $i = 0$
- While *(not converged)* do:
   - $i \leftarrow i + 1$
   - Solve:
   $$\mathbf{K}\left(\mu^{(i-1,i-1)}\right)\mathbf{U}^{(i)} - \mathbf{GP}^{(i)} = \mathbf{F}_u$$
   $$\mathbf{G}^T\mathbf{U}^{(i)} + \epsilon\mathbf{MP}^{(i)} = \mathbf{F}_p + \epsilon\mathbf{MP}^{(i-1)}$$
   - Update:
   $$\mu^{(i-1,i)} = \mu(\theta^{(i-1)}, \varepsilon(\mathbf{u}^{(i)}))$$

- Solve:
$$\mathbf{H}(\mathbf{u}^{(i)})\mathbf{\Theta}^{(i)} = \mathbf{F}_t(\mu^{(i-1,i)}, \mathbf{u}^{(i)})$$
- Update:
$$\mu^{(i,i)} = \mu(\theta^{(i)}, \varepsilon(\mathbf{u}^{(i)}))$$
- Check convergence:
If $\|\mathbf{U}^{(i)} - \mathbf{U}^{(i-1)}\| < TOL\|\mathbf{U}^{(i)}\|$ then *(converged)*

End while

*Remarks*

(1) Observe that the thermal problem is solved once the mechanical variables **U** and **P** are known for a certain iteration. There is also the possibility of swapping the order of block iterations. However, for the problems we have considered so far we have found the described option (slightly) more efficient.

(2) The iterative penalization in the above algorithm is coupled with the iterative loop used to deal with the nonlinearity of the problem. It will be seen in the numerical experiments presented below that this does not deteriorate the convergence rate of the scheme.

(3) If the viscosity does not depend on the temperature, the algorithm presented is a Picard (or successive substitution) type scheme. This is the most common option in practice [3], [16], [18], [29], [30]. In fact, convergence problems have been observed when a Newton-Raphson scheme has been employed in the type of problems we consider (see Reference [6] for further discussion and references therein).

## SMOOTHING OF ELEMENT VARIABLES

*Least-squares smoothing*

In the numerical procedure we have just described, the value of the viscosity has to be stored for each element and for each quadrature point within the element. The pressure nodal values are also located within each element. Both scalar fields will be discontinuous across interelement boundaries. For plotting purposes, it is interesting to obtain a continuous function that approximates a discontinuous one. Here, the least-squares technique employed in our calculations will be briefly described.

Let $\phi_c$ be a computed function, discontinuous across elements. A continuous function $\phi_s$ is then calculated by minimizing:

$$\|\phi_c - \phi_s\|_{L^2}^2 = \int_\Omega (\phi_c - \phi_s)^2 \, d\Omega \tag{43}$$

The function $\phi_s$ is interpolated like the components of the velocity field (or the temperature). If $N_{tp}$ is the total number of nodal points of the mesh, $N^{(i)}$ denotes the shape function associated with node $i$ and $\phi_s^{(i)}$ is the nodal value of $\phi_s$ at this point, the minimization of the functional (43) leads to the system:

$$\mathbf{M}^c \mathbf{\Phi} = \mathbf{R} \tag{44}$$

where the components of the matrix $\mathbf{M}^c$ and the vectors $\mathbf{\Phi}$ and $\mathbf{R}$ are:

$$M_{ij}^c = \int_\Omega N^{(i)} N^{(j)} d\Omega, \quad i, j = 1, ..., N_{tp} \tag{45}$$

$$\Phi_j = \phi_s^{(j)}, \quad j = 1, ..., N_{tp} \tag{46}$$

$$R_i = \int_\Omega N^{(i)} \phi_c d\Omega, \quad i = 1, ..., N_{tp} \tag{47}$$

This smoothing technique is standard [14], [31]. In order to avoid the solution of the system (44), it is usual to approximate the matrix $\mathbf{M}^c$ by a diagonal matrix $\mathbf{M}^l$. This matrix can be obtained either by the row-sum lumping technique or by using a nodal quadrature rule to evaluate the integrals in (45) and (47). In this case, the quadrature points are placed on the nodes of the element. An estimate of how well $\phi_s$ approximates $\phi_c$ can be easily obtained using standard results from interpolation theory and numerical quadrature theory.

*Nodal quadrature rules for linear and quadratic elements*

We present in Table 2 some nodal quadrature rules for the most common finite elements used in practice. Some of these rules are well known (rules 1–3, 6–11, 17 in Table 2). Our interest in obtaining the others is not their accuracy but the fact that they allow to approximate the matrix $\mathbf{M}^c$ in Eqn. (44) by a diagonal matrix, as explained above.

In Table 2, $Rn$ indicates the rule number and $Nn$ the number of nodes of the element. This is followed by a schematic description of the element that has to be precised. For both 2D and 3D elements, the bubble function is associated with a node placed in the center of the element. It is understood that the original shape functions (without the addition of the new node) have to be modified in order to have zero value at the center. Otherwise, the nodal unknown at this point would not have the meaning of being the value of the interpolated function and the matrix $\mathbf{M}^c$ would not be diagonal. For the element considered in rule number 15, bubble functions are also added in the center of the faces of the element. Elements corresponding to rules number 1, 2, 5 and 6 are triangular, tetrahedral for rules number 9, 10, 13 and 14, quadrilateral for rules number 3, 4, 7 and 8 and hexahedral for rules number 11, 12, 15 and 16.

The quadrature rule is defined by the weights of the nodes. All the nodes placed at the corners of the element have the same weight, as well as the nodes placed in the middle of the edges and in the center of the faces (in 3D elements). The values given have been normalized in such a way that their sum is 1. In the final entry of Table 2, the accuracy of the quadrature rule is given by the polynomial that can be exactly integrated. The set of polynomials of degree $n$ is denoted by $Pn$, whereas $Qn$ denotes the set of tensor-product polynomials of degree $n$ in each Cartesian direction $x, y, z$.

All the rules except rule number 5 are the best that can be obtained with the given number of quadrature points. In fact, for the 2D quadratic (simplicial) element, a second order quadrature rule is obtained if the weights are taken as 0 for the corner nodes and $\frac{1}{3}$ for the mid-side nodes. However, this rule yields a matrix $\mathbf{M}^l$, approximation of $\mathbf{M}^c$, with some zero diagonal values (those corresponding to the corner nodes). The weights given for rule number 5 have been obtained splitting the triangle into four subtriangles and applying rule number 1. It is interesting to remark that if the Richardson extrapolation is applied to rules number 1 and 5, the mentioned second order rule is recovered.

## NUMERICAL EXAMPLE

In this section we present some numerical results obtained for the well-known 4:1 plane extrusion problem. All the calculations have been carried out on a CONVEX-C120 computer using double arithmetic precision.

The geometry and the boundary conditions are depicted in Figure 1. The variation of the viscosity and the components of the velocity will be given for sections $AA$, $BB$ and $CC$ indicated in this Figure. The finite element mesh is composed of 525 $Q2/P1$ elements (biquadratic interpolation for the velocity, piecewise linear pressure), with a total of 2201 nodal points.

There are 15 elements in the $y$-direction from the coordinates $y = 3$ to $y = 4$ and only 12 from $y = 0$ to $y = 3$. The concentration of elements in the former zone is needed if one wants to reproduce accurately the shear thinning effect of fluids whose viscosity obeys the power law that we will consider:

$$\mu = K_0 \left(\sqrt{3}\hat{\varepsilon}\right)^{r-1} \exp \left(\frac{\beta}{\theta}\right) \tag{48}$$

In this expression, $K_0, r$ and $\beta$ are physical constants ($K_0$ is the material consistency and $r$ the rate sensitivity), $\theta$ is the temperature and $\hat{\varepsilon}$ is defined by:

$$\hat{\varepsilon} = \frac{2}{3} \left(\boldsymbol{\varepsilon}(\mathbf{u}) : \boldsymbol{\varepsilon}(\mathbf{u})\right)^{\frac{1}{2}} = \frac{2}{3} \left(2I_2\right)^{\frac{1}{2}}$$

where $I_2$ is the second invariant of the strain rate tensor $\boldsymbol{\varepsilon}(\mathbf{u})$. This expression is a particular case of Eqn. (13).

The values of the physical constants we have used are (all in SI units): $\rho = 1200$ (density), $c = 10$ (specific heat), $k = 2$ (thermal conduction coefficient), $K_0 = 10^6$ (material consistency) and $r = 0.2$ (rate sensitivity). For this value of $r$ the effect of the non-constant viscosity is very pronounced. Numerical experiments have also been conducted with larger values of $r$, in which case convergence is easier to achieve. Since the expression of the viscosity (48) tends to infinity when $\hat{\varepsilon}$ tends to zero, we have introduced a cut-off value $\mu_c = 10^{11}$ for $\mu$. The values of the viscosity for the converged solutions are always below this limit, except in isolated points.

Let us first discuss the performance of the iterative penalization. For values of $\beta$ between 0 and $2 \, 10^3$ the convergence history of the numerical simulation is similar. However, for larger values of $\beta$ lack of convergence can occur. We have failed to obtain converged solutions for $\beta = 5 \, 10^3$, both for the standard penalty method and for the iterative version presented in this paper. As proposed in Reference [30], under-relaxation techniques may be required when the dependence of the viscosity on the temperature is very pronounced. The convergence of the algorithm will be discussed in the case in which $\beta = 2 \, 10^3$, that is, when the viscosity depends on the temperature (thermally coupled flow).

Figure 2 shows the evolution of the discrete $L^2$ norm of the velocity residuals over the norm of the actual velocity (in %), that has been taken as the parameter to decide whether convergence has been achieved or not. Both the curves corresponding to the classical and the iterative penalty methods have been plotted. In the former case, the term $\epsilon \mathbf{MP}^{(i-1)}$ in the right-hand-side of the penalized incompressibility equation of the iterative algorithm is dropped. Here, the penalty parameter that has been used is $\epsilon = 10^{-12}$. In the first iteration, the viscosity is set to its cut-off value. Thus, the effective initial guess for the second iteration is the Newtonian solution with this viscosity. A real non-Newtonian behavior will be first uncountered in this second iteration and from there onwards iterations are required to reach the prescribed convergence tolerance. However, in Figure 2 we see that one more iteration is needed if the iterative penalization is employed. The explanation we give is that in this method the second pass of the algorithm uses the Newtonian pressures obtained in the first one, and thus the complete non-Newtonian approximation is not obtained until the third iteration. In any case, it is interesting to observe that the final convergence rate and the number of iterations needed to achieve convergence have not been deteriorated because of the iterative penalization.

The important issue is to determine how well the incompressibility constraint has been approximated. If we denote by $\mathbf{B}$ the discrete divergence matrix, we should have $\|\mathbf{BU}\| = 0$ in the real incompressible case. The evolution of $\|\mathbf{BU}\|$ as the iterative procedure goes on has been plotted in Figure 3 (we have *not* normalised this norm by dividing it by $N_{tp}^{\frac{1}{2}}$, as it is done sometimes). Observe that this value keeps constant for the classical penalty method and that it decreases uniformly up to a value of order $10^{-10}$ in 14 iterations if the iterative penalization is

used. One might think that the value of order $10^{-6}$ obtained with the classical penalty method is a good enough approximation. However, this may be somehow misleading, since the smallest value of the final viscosity, say $\mu_1$, is of order $10^3$, and thus $\epsilon \approx 10^{-9}\mu_1^{-1}$ whereas the largest viscosity value, say $\mu_2$, is of order $10^9$ and then $\epsilon \approx 10^{-3}\mu_2^{-1}$. Thus, the parameter $\bar{\epsilon}$ introduced earlier is of order $10^{-9}$ in the low viscosity zones and of order $10^{-3}$ in the high viscosity zones. Recalling that the approximation of the incompressibility constraint is driven by $\bar{\epsilon}$, we may expect a much better satisfaction of this constraint in the low viscosity regions than in the zones where the viscosity is high. If smaller penalty parameters are employed, the solution is affected by the ill-conditioning of the stiffness matrix, even for the direct solver we use. For $\epsilon = 10^{-16}$ this ill-conditioning is so important that the algorithm fails to converge.

The same experiments discussed above have been performed using a penalty parameter $\epsilon = 10^{-9}$ and the results are presented in Figures 4 (convergence history) and 5 (evolution of the $L^2$ norm of the discrete divergence). The conclusions are similar to the previous case. Observe now that oscillations are found for the first 5 iterations and then the iterates converge uniformly. The reason for this behavior is the high value of $\epsilon$, that is of the same order as $\mu_2^{-1}$, the inverse of the maximum viscosity, and 100 times higher than $\mu_c^{-1}$, the inverse of the cut-off value.

The physical results for this problem are presented if Figures 6 through 16 (coordinates are given in decimeters). Figure 6 shows the streamlines for $\beta = 0$ (thermally uncoupled flow) and Figure 7 for $\beta = 2\ 10^3$, where the effect of the temperature on the viscosity (and thus on the velocity) is apparent. The temperature contours are plotted in Figure 8. From Eqns. (4) and (5) it is clear that the temperature will rise where the internal mechanical work is higher, that is, in the zones with high strain rate. This happens near the corner $(x, y) = (16, 3)$. Figures 9,10 and 11 show the variation of the viscosity along the sections $AA$, $BB$ and $CC$ indicated in Figure 1. The approximation in the $AA$ section is not very good for $0 \leq y \leq 3$. As it has been already said, the discretization there is poor. However, the variation of the $x-$ and $y-$velocity components (Figures 12 and 15) is smooth, since the shear thinning effect is not important in this section.

## CONCLUSIONS

In this paper, a numerical procedure for the finite element solution of viscous non-Newtonian creeping flows using the penalty method has been discussed. We have seen that the classical approach is not appropriate when the viscosity is variable, since either the incompressibily constraint is poorly approximated or the stiffness matrix is ill-conditioned. This problem is circumvented if the iterative penalization presented here is used. The method has been motivated and analyzed for Newtonian fluids, although numerical experiments have demonstrated that the *ad hoc* extension to non-linear fluids, whose analysis escapes us, is an effective remedy for the mentioned problems.

The motivation has been based on a residual argument, valid for nonlinear problems and for cases in which the stiffness matrix is not symmetric. The analysis for the linear problem also explains why the penalty parameter $\epsilon$ must be taken proportional to the inverse of the viscosity.

Some other related issues have also been treated, such as the block iterative scheme used to couple the thermal and the mechanical problems and the smoothing technique utilized in order to obtain continuous viscosity and pressure fields. Nodal quadrature rules for the most common finite elements used in practice have also been given to apply effectively this method.

## APPENDIX

In order to get more insight on the iterative penalty method when dealing with nonlinear problems, we consider here the system of equations

$$A(x)x + By = f$$
$$B^T x \quad\quad = 0$$
(49)

where $x$ and $y$ are vectors of nodal unknowns (the bold notation has been abandoned) and $A$ and $B$ are matrices, the former depending on the unknown $x$.

For simplicity, we assume that system (49) is solved by using the simplest fixed-point or Picard scheme. Let $(x^{(i-1)}, y^{(i-1)})$ be a given guess for $(x, y)$. The differences between this guess and the exact solution, $\delta x := x - x^{(i-1)}$, $\delta y := y - y^{(i-1)}$, will be the solution of

$$A(x^{(i-1)} + \delta x)\delta x + B\delta y = f - A(x^{(i-1)} + \delta x)x^{(i-1)} - By^{(i-1)}$$
$$B^T \delta x \quad\quad = -B^T x^{(i-1)}$$
(50)

The main idea behind the Picard scheme is to approximate $A(x^{(i-1)} + \delta x) \approx A(x^{(i-1)})$. Thus, we are led to

$$A(x^{(i-1)})\delta\bar{x} + B\delta\bar{y} = f - A(x^{(i-1)})x^{(i-1)} - By^{(i-1)}$$
$$B^T \delta\bar{x} \quad\quad = -B^T x^{(i-1)}$$
(51)

$\delta\bar{x}$ and $\delta\bar{y}$ being approximations to $\delta x$ and $\delta y$, respectively. The second step now is to solve for $\delta\bar{x}$ and $\delta\bar{y}$ using the penalty method. With the notation used in the main text, we will have to find $\delta\bar{x}^\epsilon$ and $\delta\bar{y}^\epsilon$ such that

$$A(x^{(i-1)})\delta\bar{x}^\epsilon + B\delta\bar{y}^\epsilon = f - A(x^{(i-1)})x^{(i-1)} - By^{(i-1)}$$
$$B^T \delta\bar{x}^\epsilon + \epsilon M \delta\bar{y}^\epsilon \quad = -B^T x^{(i-1)}$$
(52)

If we define $x^{(i)} := x^{(i-1)} + \delta\bar{x}^\epsilon$, $y^{(i)} := y^{(i-1)} + \delta\bar{y}^\epsilon$, system (52) may be re-written as

$$A(x^{(i-1)})x^{(i)} + By^{(i)} = f$$
$$B^T x^{(i)} + \epsilon M y^{(i)} \quad = \epsilon M y^{(i-1)}$$

that is, the Picard algorithm has been coupled with the iterative penalization. So, we see that the two steps used to arrive from the original system (50) to (52) are

(i) Approximate $A(x^{(i-1)} + \delta x) \approx A(x^{(i-1)})$.
(ii) Solve *for the increments* using the penalty method.

It is clear that whenever the algorithm be convergent, it will converge towards the solution of (49). On the other hand, if the classical penalty method is employed system (49) has to be modified *a priori*. In this approach, step (ii) in the above development is clearly missing.


## REFERENCES

[1] J. Baranger and K. Najib. Analyse numérique des écoulements quasi-Newtoniens dont la viscosité obéit à la loi puissance ou à la loi de carreau. *Numer. Math.*, vol. 58, 35–49 (1990)

[2] F. Brezzi and K.J. Bathe. A discourse on the stability conditions for mixed finite element formulations. *Comp. Meth. in Appl. Mech. and Engng.*, vol. 82, 27–57 (1990)

[3] G.F. Carey, K.C. Wang and W.C. Joubert. Performance of iterative methods for Newtonian and generalized Newtonian flows. *Int. J. Num. Meth. in Fluids*, vol. 9, 127–150 (1989)

[4] A.J. Chorin. A numerical method for solving incompressible viscous flow problems. *J. Comp. Phys.*, vol. 2, 12–26 (1967)

[5] R. Codina. An iterative penalty method for the finite element solution of the stationary Navier-Stokes equations. *CIMNE Report Num. 12* (1991)

[6] C. Cuvelier, A. Segal and A. van Steenhoven. *Finite element methods and Navier-Stokes equations.* (Reidel, 1986)

[7] M.S. Engelman, R.L. Sani, P.M. Gresho and M. Bercovier. Consistent vs reduced integration penalty methods for incompressible media using several old and new elements. *Int. J. Num. Meth. in Fluids*, vol. 2, 25–42 (1983)

[8] C.A. Felippa. Iterative procedures for improving penalty function solutions of algebraic systems. *Int. J. Num. Meth. in Engng.*, vol. 12, 821–836 (1978)

[9] M. Fortin. Old and new finite elements for incompressible flows. *Int. J. Num. Meth. in Fluids*, vol. 3, 347–364 (1981)

[10] M. Fortin and S. Boivin. Iterative stabilization of the bilinear velocity-constant pressure element. *Int. J. Num. Meth. in Fluids*, vol. 10, 125–140 (1990)

[11] V. Girault and P.A. Raviart. *Finite element methods for Navier-Stokes equations* (Springer-Verlag, 1986).

[12] R. Glowinski. *Numerical methods for nonlinear variational problems.* (Springer-Verlag, 1984)

[13] J.C. Heinrich and B.R. Dyne. On the penalty method for incompressible fluids. In *Finite elements in the 90's*, E. Oñate, J. Periaux and A. Samuelson, Eds. (Springer-Verlag/CIMNE, Barcelona 1991)

[14] T.J.R. Hughes. *The finite element method. Linear static and dynamic analysis.* (Prentice-Hall, 1987)

[15] T.J.R. Hughes, W.K. Liu and A. Brooks. Finite Element Analysis of Incompressible Viscous Flows by the Penalty Function Formulation. *J. Comp. Phys.*, vol. 30, 1–60 (1979)

[16] P. Hurez, P.A. Tanguy and F.H. Bertrand. A finite element analysis of die swell with pseudoplastic and viscoplastic fluids. *Comp. Meth. in Appl. Mech. and Engng.*, vol. 86, 87–103 (1991)

[17] C. Johnson and J. Pitkaranta. Analysis of some mixed finite element methods related to reduced integration. *Math. of Comp.*, vol. 38, 375–400 (1982)

[18] T.J. Liu, H.M. Lin and C.N. Hong. Comparison of two numerical methods for the solution of non-Newtonian flow in ducts. *Int. J. Num. Meth. in Fluids*, vol. 8, 845–861 (1988)

[19] D.S. Malkus and T.J.R. Hughes. Mixed finite element methods-reduced and selective integration techniques: a unification of concepts. *Comp. Meth. in Appl. Mech. and Engng.*, vol. 15, 63–81 (1978)

[20] J.C. Nagtegaal, D.M. Parks and J.R. Rice. On numerically accurate finite element solutions in the fully plastic range. *Comp. Meth. in Appl. Mech. and Engng.*, vol. 4, 153–177 (1974)

[21] J.T. Oden. RIP-methods for Stokesian flows. In *Finite elements in fluids*, vol. 4, R.H. Gallagher, D.H. Norrie, J.T. Oden and O.C. Zienkiewicz (eds.) John Wiley & Sons Ltd. (1982)

[22] J.T. Oden, N. Kikuchi and Y.J. Song. Penalty-finite element methods for the analysis of Stokesian flows. *Comp. Meth. in Appl. Mech. and Engng.*, vol. 31, 297–329 (1982)

[23] M.P. Robichaud, P. Tanguy and M. Fortin. An iterative implementation of the Uzawa algorithm for 3-D fluid flow problems. *Int. J. Num. Meth. in Fluids*, vol. 10, 429–442 (1990)

[24] E.M. Salonen. An iterative penalty function method in structural analysis. *Int. J. Num. Meth. in Engng.*, vol. 10, 413–421 (1976)

[25] P. Le Tallec and V. Ruas. On the convergence of the bilinear-velocity constant-pressure finite element method in viscous flow. *Comp. Meth. in Appl. Mech. and Engng.*, vol. 54, 235–243 (1986)

[26] R. Temam. *Navier-Stokes equations.* (North-Holland, 1984)

[27] E. Thompson. Use of pseudo-concentrations to follow creeping viscous flows during transient analysis. *Int. J. Num. Meth. in Fluids*, vol. 6, 749–761 (1988)

[28] E. Thompson and R.E. Smelser. Transient analysis of forging operations by the pseudo-

concentration method. *Int. J. Num. Meth. in Engng.*, vol. 25, 177–189 (1988)

[29] O.C. Zienkiewicz, P.C. Jain and E. Oñate. Flow of solids during forming and extrusion: some aspects of numerical solution. *Int. J. Num. Meth. in Engng.*, vol. 14, 15–38 (1978)

[30] O.C. Zienkiewicz, E. Oñate and J.C. Heinrich. A general formulation for coupled thermal flow of metals using finite elements. *Int. J. Num. Meth. in Engng.*, vol. 17, 1497–1514 (1981)

[31] O.C. Zienkiewicz and R.L. Taylor. *The Finite Element Method*, Fourth Edition, Vol. 1 (McGraw-Hill, 1989)

[32] O.C. Zienkiewicz, R.L. Taylor and J.M. Too. Reduced integration technique in general analysis of plates and shells. *Int. J. for Numer. Meth. in Engng.*, vol. 3, 275–290 (1971)

[33] O.C. Zienkiewicz, J.P. Vilotte, S. Toyoshima and S. Nakazawa. Iterative method for constraint and mixed approximation; an inexpensive improvement of F.E.M. performance. *Comp. Meth. in Appl. Mech. and Engng.*, vol. 51, 3–29 (1985)

## LIST OF TABLES

## LIST OF FIGURES

Table 1. Some stable finite elements
for the Stokes problem

| Element | Nnu (2/3D) | Nnp (2/3D) | Description |
|---------|------------|------------|-------------|
| Q1/P0 | 4/8 | 1/1 | Continuous bi or tri-linear velocity. Piecewise constant pressure. |
| Q2/P1 | 9/27 | 3/4 | Continuous bi or tri-quadratic velocity. Piecewise linear pressure. |
| Q2-/P0 | 8/20 | 1/1 | Serendipid velocity interpolation. Piecewise constant pressure. |
| P2+/P0 | 7/15 | 3/4 | Continuous quadratic velocity enriched with bubble functions. Piecewise linear pressure |
| P2/P0 | 6/10 | 1/1 | Continuous quadratic velocity. Piecewise constant pressure. |

Table 2. Nodal quadrature rules for linear
and quadratic finite elements

| Rn | Nn | Description | Weights | | | | Polynomial |
|----|----|-------------|---------|-------|-------|--------|------------|
|    |    |             | Corners | Edges | Faces | Center |            |
| **2D Elements** | | | | | | | |
| 1 | 3 | Linear | 1/3 | | | | P1 |
| 2 | 4 | Linear+bubble | 1/12 | | | 3/4 | P2 |
| 3 | 4 | Bilinear | 1/4 | | | | Q1 |
| 4 | 5 | Bilinear+bubble | 1/12 | | | 2/3 | P2 |
| 5 | 6 | Quadratic | 1/12 | 1/4 | | | P1 |
| 6 | 7 | Quad.+bubble | 1/20 | 2/15 | | 9/20 | P3 |
| 7 | 8 | Serendipid | $-1/12$ | 1/3 | | | P2 |
| 8 | 9 | Biquadratic | 1/36 | 1/9 | | 4/9 | Q3 |
| **3D Elements** | | | | | | | |
| 9 | 4 | Linear | 1/4 | | | | P1 |
| 10 | 5 | Linear+bubble | 1/20 | | | 4/5 | P2 |
| 11 | 8 | Trilinear | 1/8 | | | | Q1 |
| 12 | 9 | Trilin.+bubble | 1/24 | | | 2/3 | P2 |
| 13 | 10 | Quadratic | $-1/120$ | 1/5 | | | P2 |
| 14 | 11 | Quad.+bubble | 1/160 | 1/15 | | 8/15 | P3 |
| 15 | 15 | Quad.+bubble +face bubbles | 17/840 | 4/105 | 27/280 | 32/105 | P3 & terms $x^2$ $yz$,... |
| 16 | 20 | Serendipid | $-1/8$ | 1/6 | | | P2 |
| 17 | 27 | Triquadratic | 1/216 | 1/54 | 2/27 | 8/27 | Q3 |
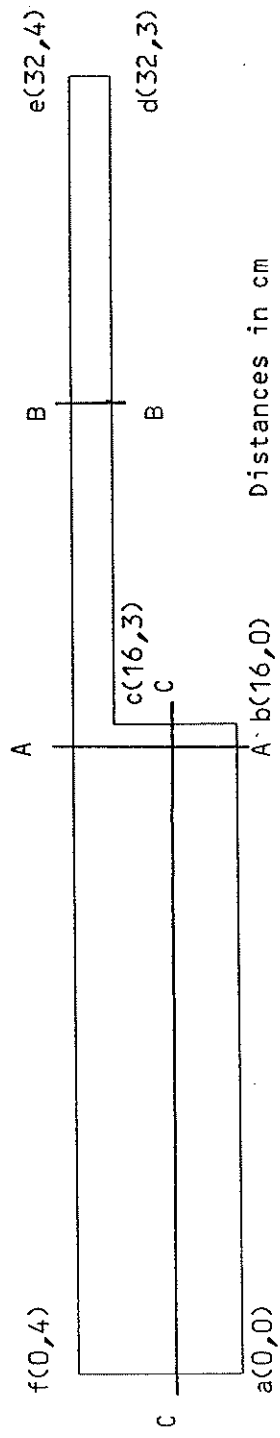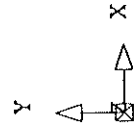
**Figure 1.** Geometry and boundary conditions for the 4:1 plane extrusion problem.
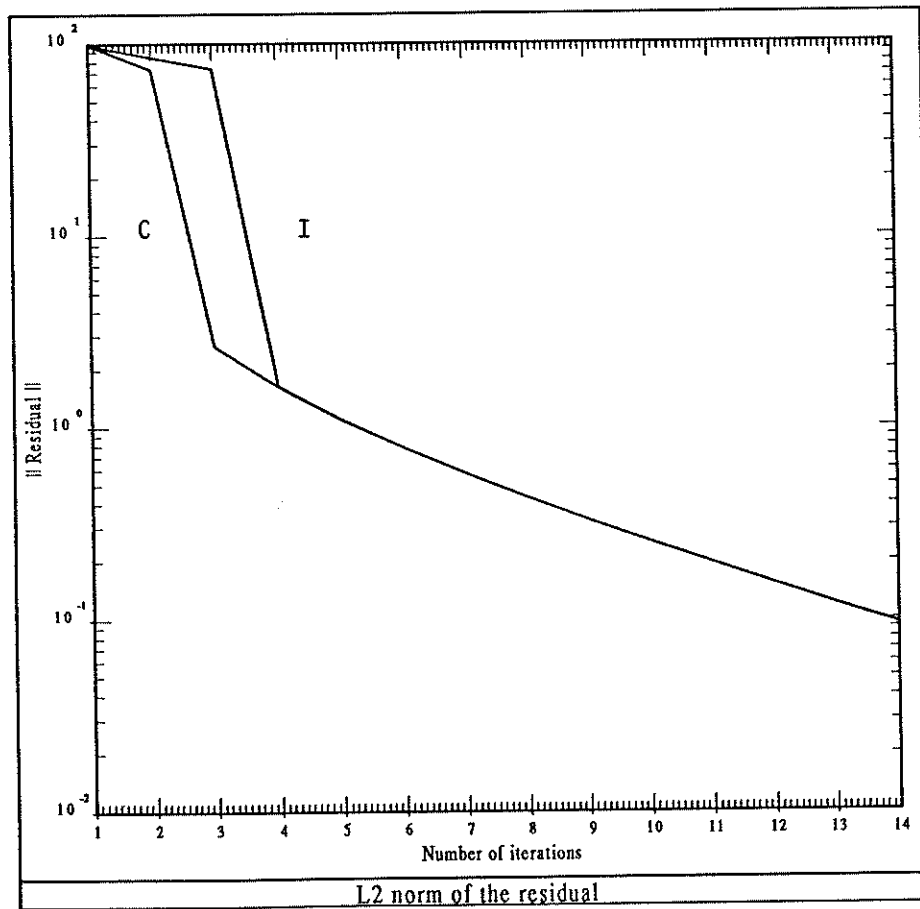
**Figure 2.** Convergence history for $\epsilon = 10^{-12}$. Classical (C) and iterative (I) penalty methods.
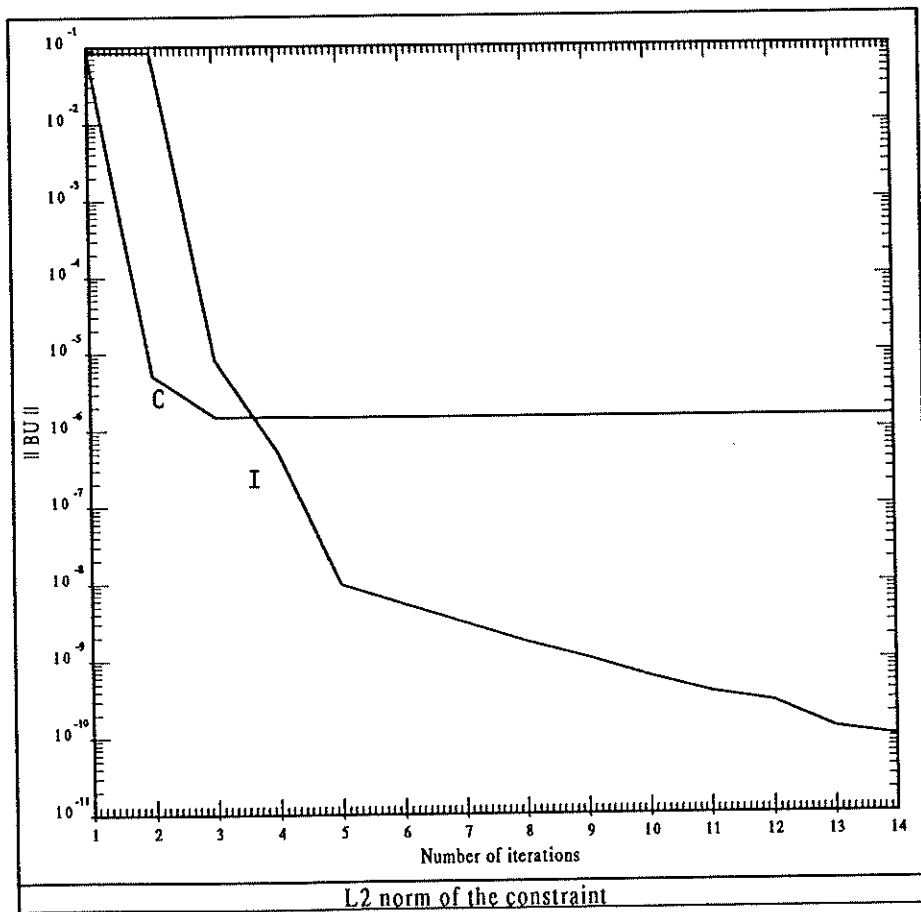
**Figure 3.** Evolution of the norm of the discrete divergence for $\epsilon = 10^{-12}$. Classical (C) and iterative (I) penalty methods.
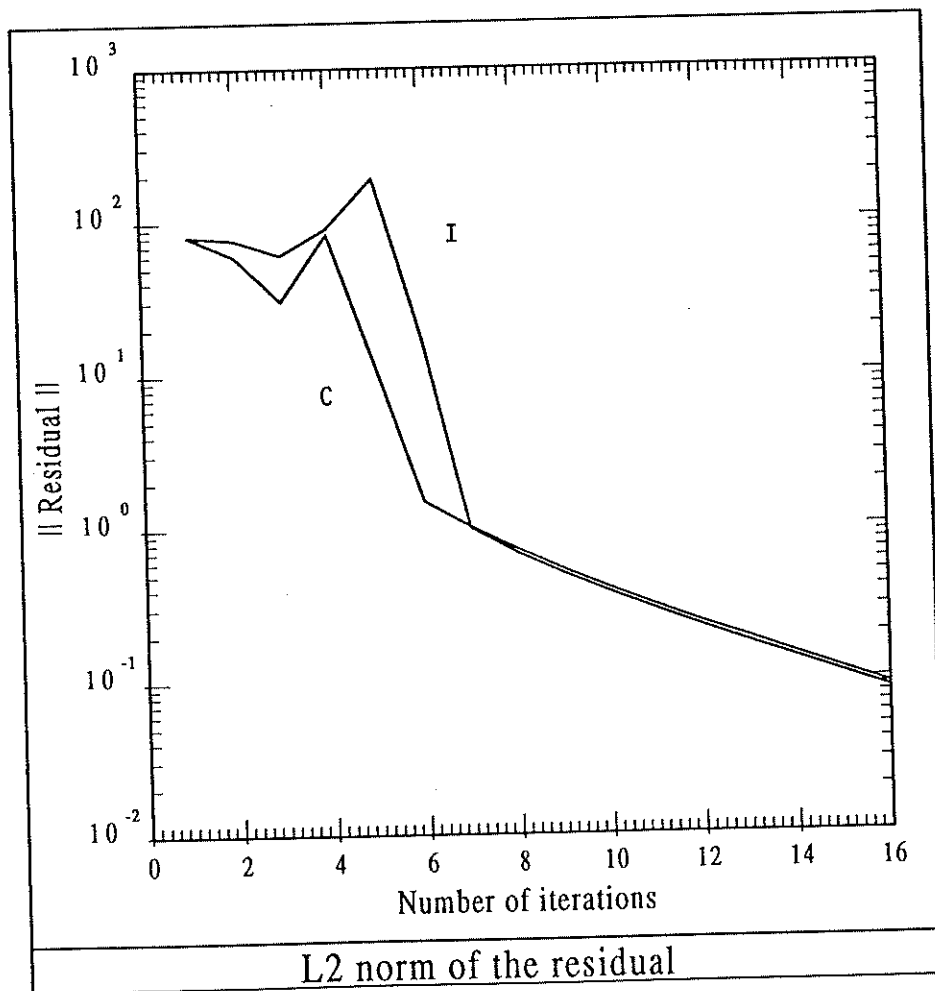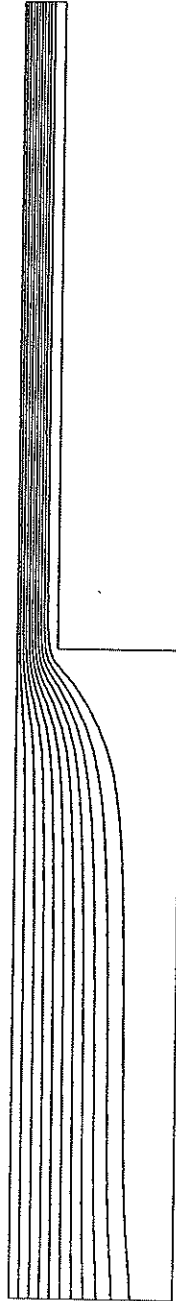
**Figure 4.** Convergence history for $\epsilon = 10^{-9}$. Classical (C) and iterative (I) penalty methods.
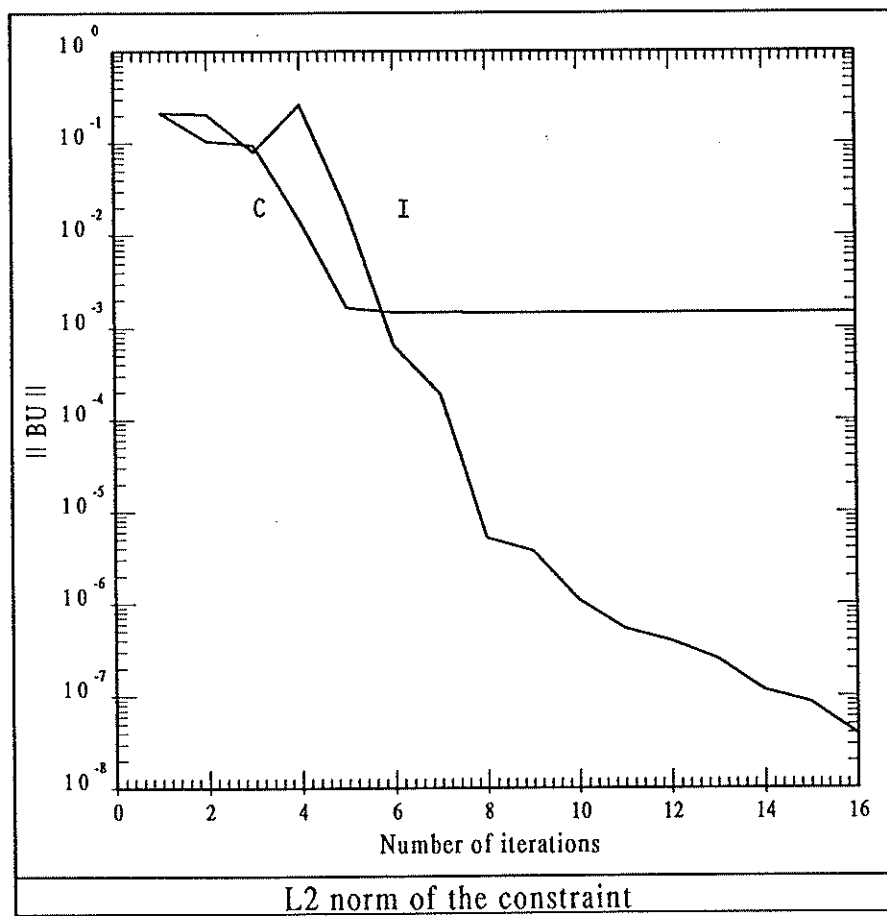
**Figure 5.** Evolution of the norm of the discrete divergence for $\epsilon = 10^{-9}$. Classical (C) and iterative (I) penalty methods.

**Figure 6.** Streamfuction contours for $\beta = 0$.
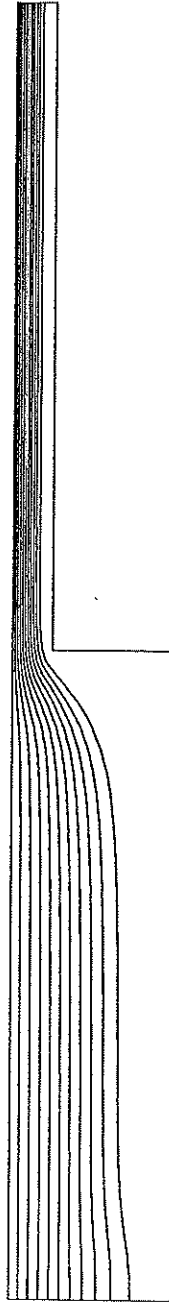
**Figure 7.** Streamfuction contours for $\beta = 2 \; 10^3$.
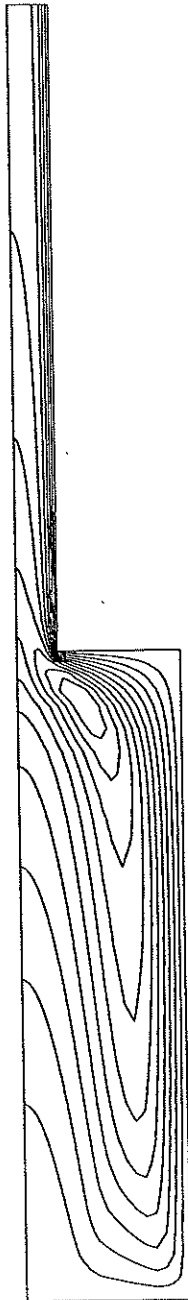
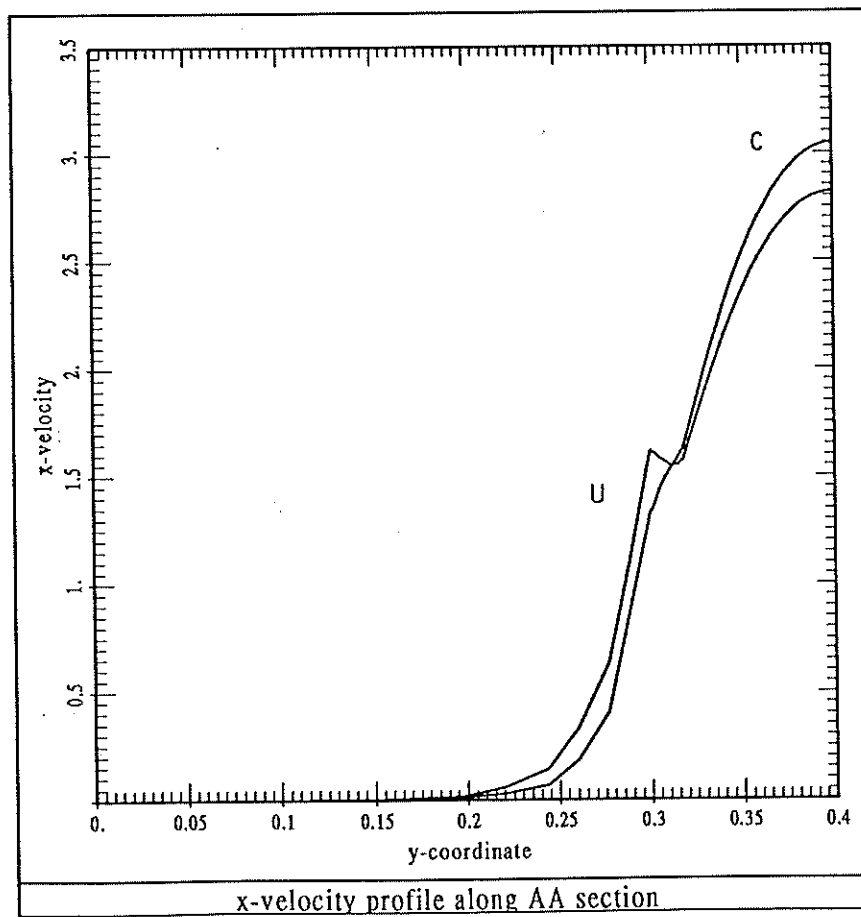**Figure 8.** Temperature contours for $\beta = 2 \ 10^3$.
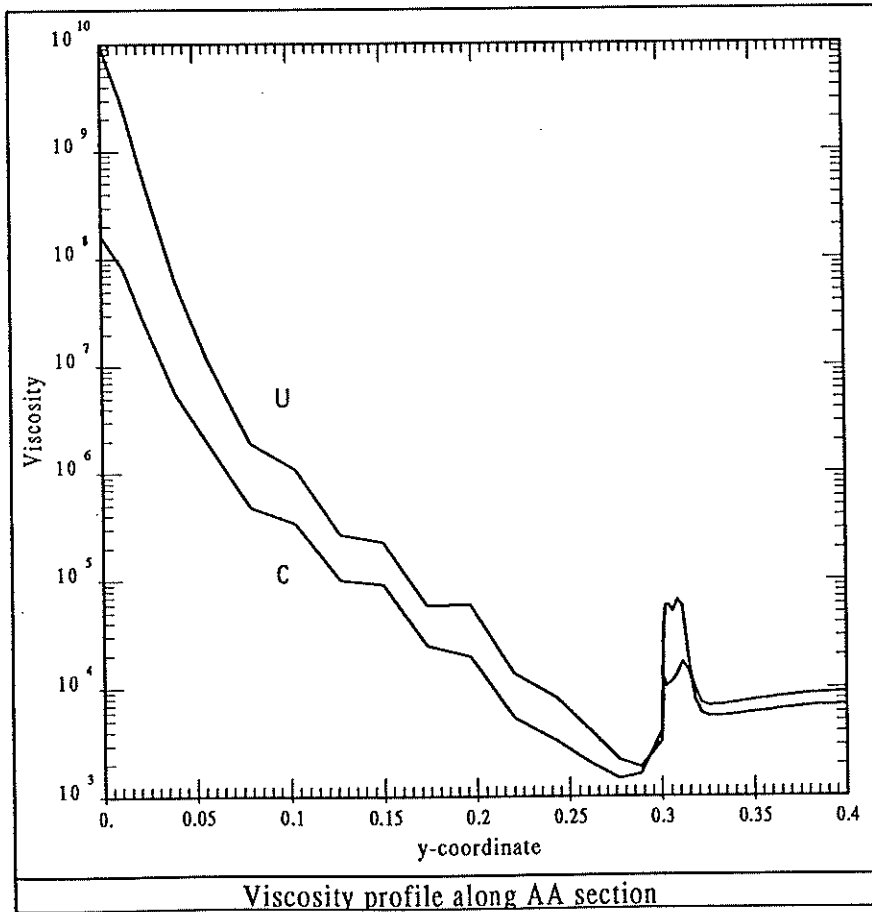
**Figure 9.** Viscosity variation along $AA$ section. $\beta = 0$ (U) and $\beta = 2 \ 10^3$ (C).
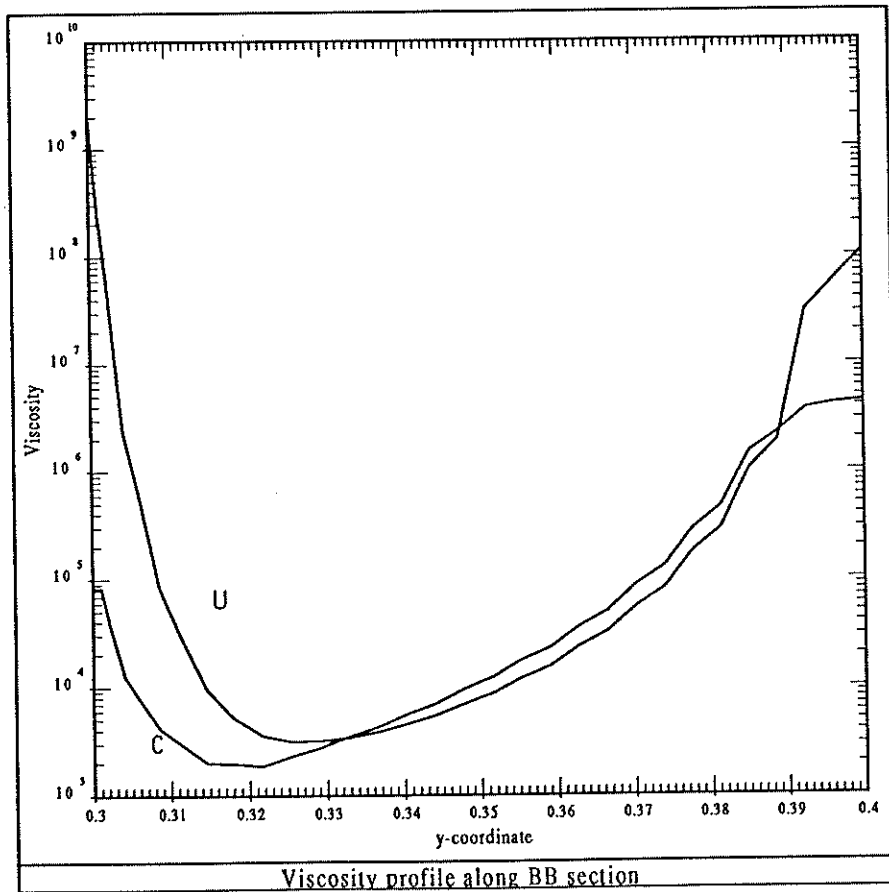
Figure 10. Viscosity variation along $BB$ section. $\beta = 0$ (U) and $\beta = 2\ 10^3$ (C).
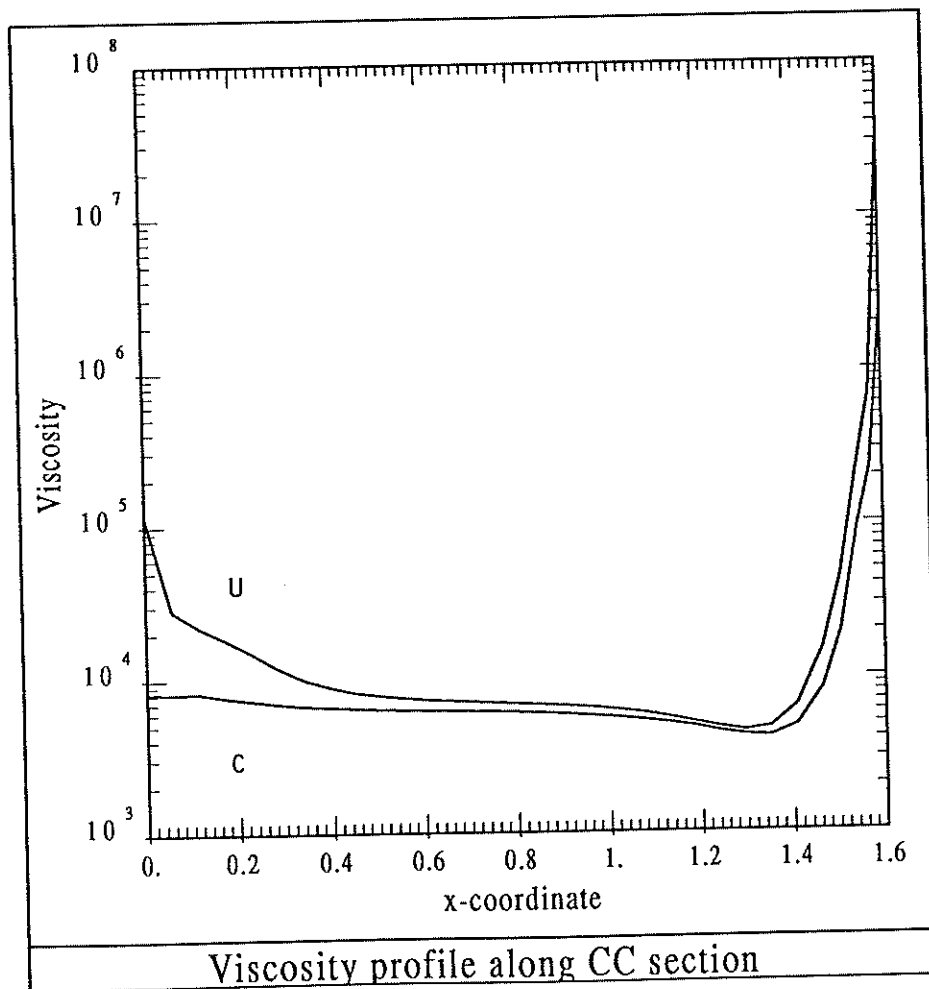
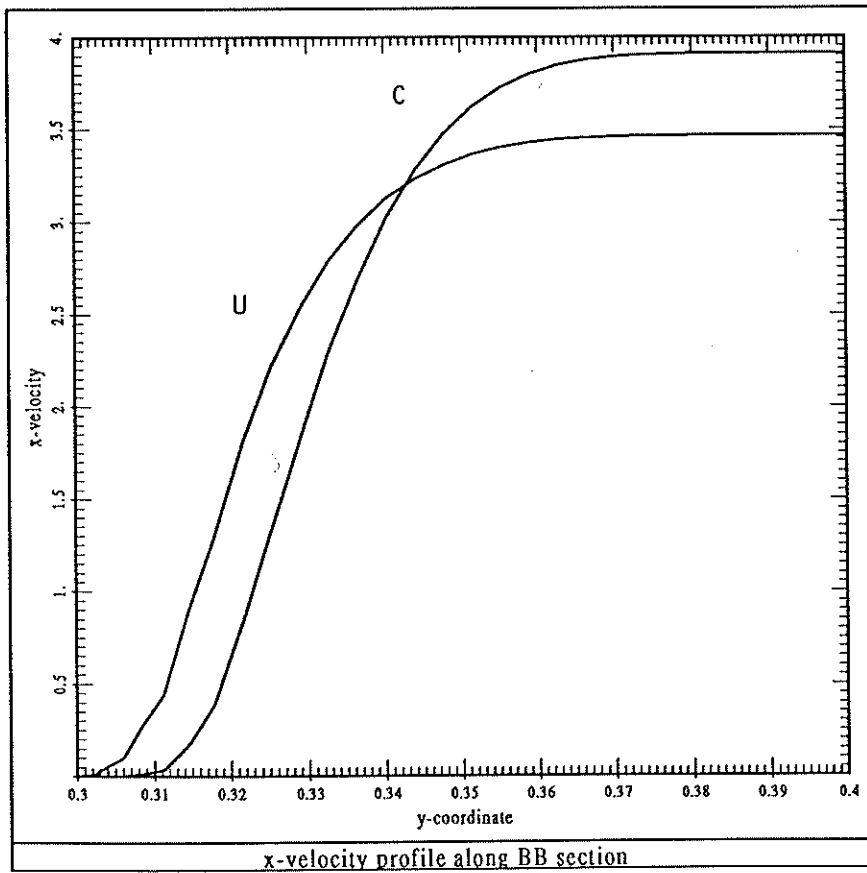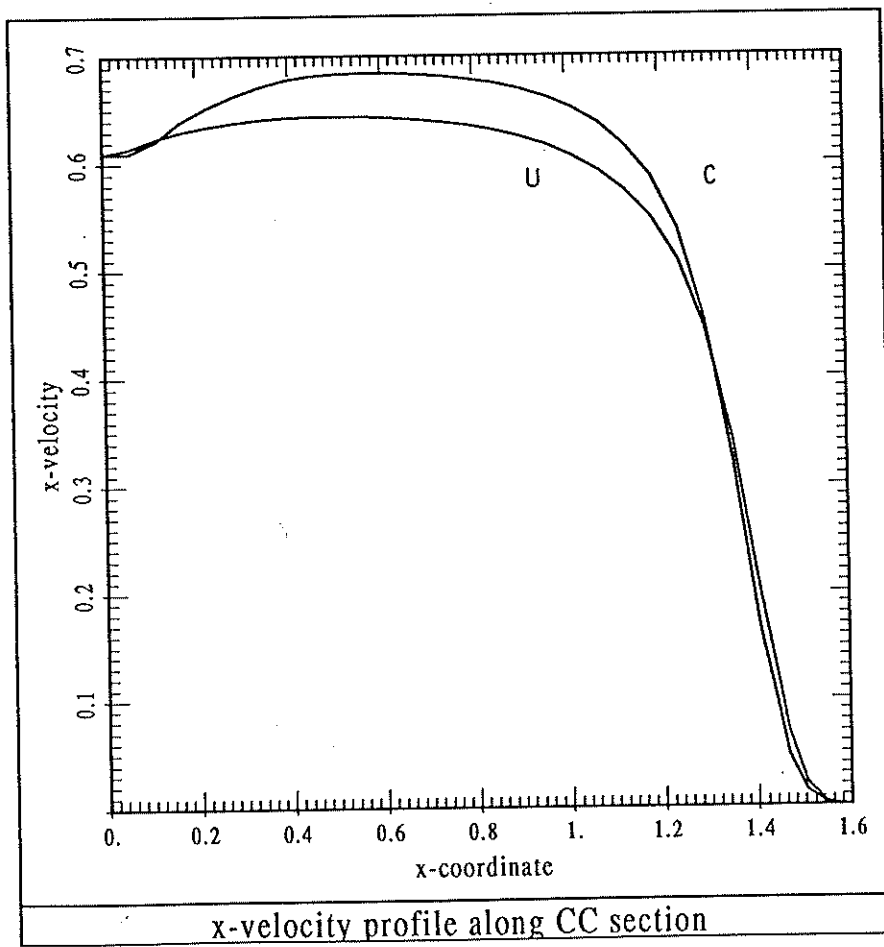**Figure 11.** Viscosity variation along $CC$ section. $\beta = 0$ (U) and $\beta = 2\ 10^3$ (C).

**x-velocity profile along AA section**

**Figure 12.** $x$–velocity variation along $AA$ section. $\beta = 0$ (U) and $\beta = 2 \ 10^3$ (C).

31

**Figure 13.** $x$–velocity variation along $BB$ section. $\beta = 0$ (U) and $\beta = 2 \ 10^3$ (C).
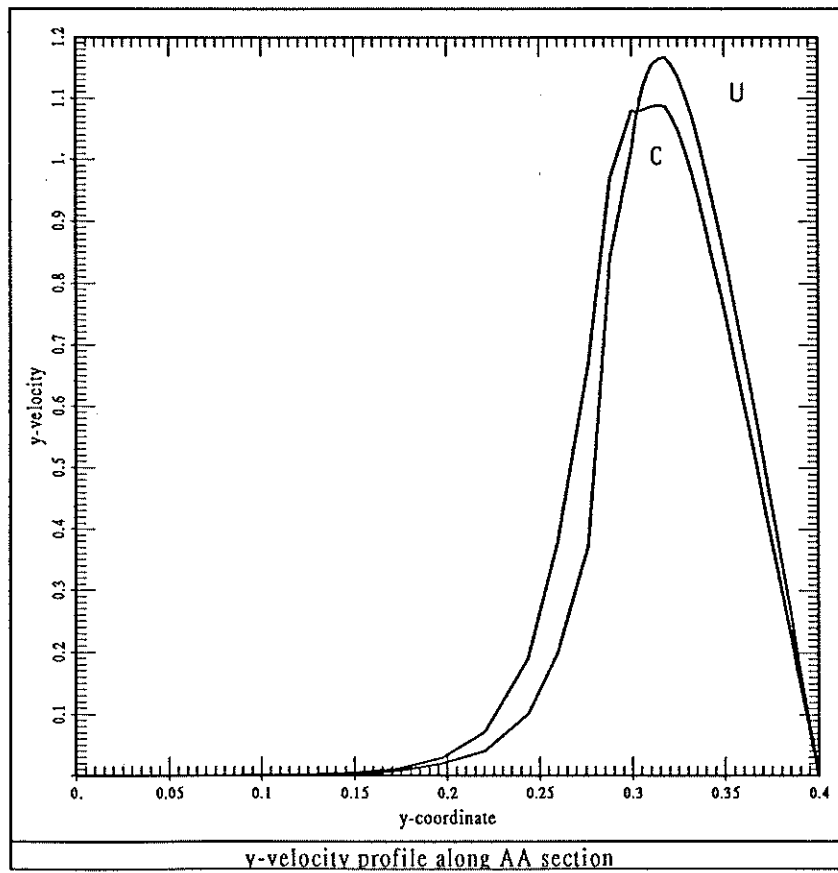
x-velocity profile along CC section

**Figure 14.** $x-$velocity variation along $CC$ section. $\beta = 0$ (U) and $\beta = 2\ 10^3$ (C).

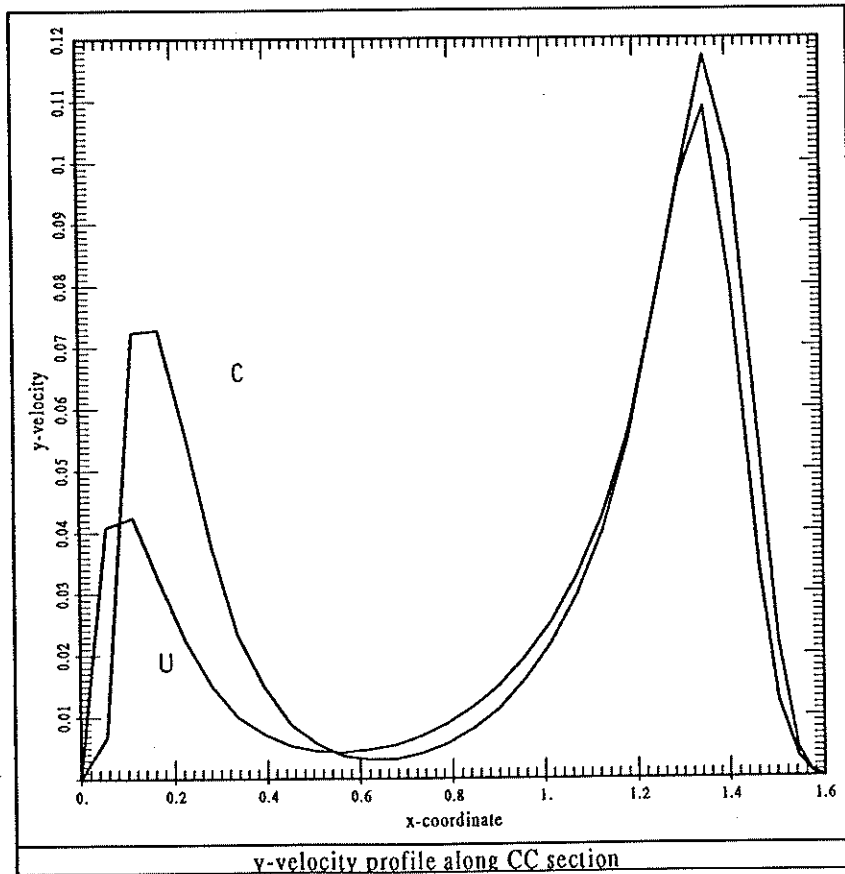**Figure 15.** $y$−velocity variation along $AA$ section. $\beta = 0$ (U) and $\beta = 2 \; 10^3$ (C).

**Figure 16.** $y-$velocity variation along $CC$ section. $\beta = 0$ (U) and $\beta = 2 \; 10^3$ (C).